Phys Chem Minerals (2004) 31: 532–542
DOI 10.1007/s00269-004-0408-9
© Springer-Verlag 2004

ORIGINAL PAPER

K. Shimoda · M. Okuno · Y. Syono · M. Kikuchi
K. Fukuoka · M. Koyano · S. Katayama

Structural evolutions of an obsidian and its fused glass by shock-wave compression

Received: 7 July 2003 / Accepted: 22 May 2004

Abstract Shock-recovery experiments for obsidian and its fused glass have been carried out with pressure up to 35 GPa. Structural evolution accompanying the shock compression was investigated using X-ray diffraction technique, Raman and infrared spectroscopy. The densities of obsidian and its fused glass increased with applied shock pressure up to ~25 GPa. Densification reached a maximum of 4.7 and 3.6% for obsidian and its fused glass, respectively. The densification mechanism is attributed to reduction of the T–O–T angle, and changes in ring statistics in the structure. Density reduction observed at greater than 25 GPa of applied shock pressure is due to partial annealing of the high-density glass structures brought by high post-shock residual temperature. The density of fused glass is almost equal to its original value at 35 GPa while the shocked obsidian has a slightly lower value than its original value. Amorphization of crystallites present in the obsidian due to shock compression is probably the cause of the density decrease. The structural evolution observed in shock-compressed obsidian and its fused glass can be explained by densification resulting from average T–O–T angle reduction and increase of small rings, and subsequent structural relaxation by high post-shock temperature at applied shock compression above ~25 GPa.

Keywords Obsidian · Shock compression · Densified glass · Crystallite

K. Shimoda (✉) · M. Okuno
Department of Earth Science, Faculty of Science,
Kanazawa University, Kanazawa, 920-1192, Japan
E-mail: ruby@earth.s.kanazawa-u.ac.jp
Fax: +8176-264-5746

Y. Syono · M. Kikuchi · K. Fukuoka
Institute for Materials Research. Tohoku University,
Sendai, 980-8577, Japan

M. Koyano · S. Katayama
School of Materials Science,
Japan Advanced Institute of Science and Technology,
923-1292, Japan

Introduction

Studies on the structural changes of silicate glasses and crystals undergone during shock-wave compression are important in understanding the formation of tektite, impactite, or diaplectic glass and in estimating the shock pressure during a shock event. The mechanisms of densification and relaxation during the structural evolution of silicate glasses under dynamic compression can be known through shock experiments. Several authors have already investigated the structural evolution in shock-densified SiO_2 glass (Okuno et al. 1999; Shimada et al. 2002), anorthite ($CaAl_2Si_2O_8$) glass (Reynard et al. 1999) and albite ($NaAlSi_3O_8$) glass (Takabatake 2000). It has been consistently reported in these studies that densification of glasses increases rapidly with shock pressure above 15 GPa and reaches a maximum at 24–26 GPa before undergoing a steep retrace at even higher shock pressures. The densification mechanisms of the glasses were attributed to the reduction of the T–O–T angle with the formation of small rings of TO_4 tetrahedra.

Tektites are naturally occuring glasses scattered over wide areas. Previous studies have identified the compositional and structural similarities of tektites and volcanic glasses (White and Minser 1984; Wright et al. 1984; Heide et al. 2001). There has been no clear information in previous studies regarding the origin of tektites, making its possible origin controversial. Gibbons and Ahrens (1971) reported an increase in the refractive index of tektite glass by shock compression applied up to 13.3 GPa. The shock-wave equations of state for natural rhyolite (Anderson et al. 1998) and basalt (Nakazawa et al. 1997) have also been determined. Further shock compression studies for silicate glasses with more complex compositions are necessary to elucidate the formation of tektites.

Based on X-ray diffraction technique and a quasi-crystalline model, Hochella and Brown (1984) suggested a modifier-cation-stuffed structural framework for

rhyolitic glass. This proposed structural model, which consists of six-membered rings of SiO_4 and AlO_4 tetrahedra with interstitial modifier ions, gained support from Zotov et al. (1989). Okuno et al. (1998) attributed the 9% permanent densification in volcanic glass resulting from hydrostatic compression (4 GPa and 500 °C) to reduction of ring size in the framework structure.

A detailed study of the structural evolution and the densification mechanisms of volcanic glass with a complex composition such as obsidian using shock compression is performed in the present study. X-ray diffraction, Raman, and infrared (IR) spectroscopic techniques were used to investigate the structural changes in obsidian and its fused glass. Results in this study are further compared with the structural evolutions discussed in previous studies. The influence of crystallites on the shock behavior of obsidian is also considered.

Experimental

Specimen

Microscopically homogeneous obsidian from Krafla, Iceland, was used in this study. A scanning electron microscope (SEM, Topocon Alpha at 30 mA and 20 kV) with an energy-dispersive X-ray (EDX) analyzer was used to analyze the chemical composition of the obsidian. Several analysis points were selected and averaged. The chemical composition of the obsidian is summarized in Okuno et al. (1998) and shown in Table 1. The calculated CIPW norm showed quartz (39.4 wt%), albite (33.8 wt%), orthoclase (16.6 wt%), anorthite (6.5 wt%), and other minerals in small quantities.

To determine the contribution of crystallites in the shock behavior of obsidian, crystallite-free fused obsidian was prepared. Obsidian blocks were placed in a Pt crucible heated by an electric furnace to 1650 °C for 3 h and quenched in air to room temperature. The preparation of the crystallite-free obsidian was done under ambient pressure.

Shock-wave experiments and density measurements

Shock-wave experiments were performed using a single-stage propellant gun, which has a 25-mm bore and 4-m length (Goto and Syono 1984), at the Institute for Materials Research in Tohoku University. The obsidian and its fused glass were cut into thin disks (10 mm in diameter, 2 mm in thickness) and encased in a stainless steel container. A stainless steel flyer hits the specimen container at velocities up to about 1.6 km s^{-1}. Shock pressures achieved, based on estimates from the measured projectile velocities (i.e., impedance matching method), were 16.3, 21.7, 24.3, 31.0, and 36.8 GPa for obsidian, and 15.2, 19.4, 25.9, 30.9, and 35.1 GPa for the fused glass. The precision of the estimated shock pressures is 0.1 GPa. Obsidian specimens that have undergone shock pressures at 16.3 and 21.7 GPa, and the fused glass at 15.2 and 19.4 GPa shock were powdered aggregates. The others recovered were semitransparent blocks.

The differences in densities between samples that have undergone shock compression and the original samples were determined by immersing the samples in a mixture of CH_2I_2 and acetone. Measurements were repeated six times or more for each sample.

Table 1 Chemical composition of the obsidian from Krafla, Iceland. (Okuno et al. 1998)

Composition	Wt%
SiO_2	76.17
Al_2O_3	12.27
Na_2O	3.99
FeO*[a]	3.29
K_2O	2.82
CaO	1.69
TiO_2	0.30
P_2O_5	0.29
MnO	0.11
Cr_2O_3	0.06
NiO	0.01
Total	101.00

[a] FeO* represents total iron

X-ray diffraction measurements

The X-ray diffraction measurements were performed using a four-circle X-ray diffractometer (Rigaku AFC-7s) with MoKα radiation monochromated by pyrolytic graphite. Scan step was set at 0.5 ° in 2θ range of 5–120 °, corresponding to 0.77–15.3 $Å^{-1}$ in $S = 4\pi\sin\theta/\lambda$. These diffraction data were used for the calculation of radial distribution function. Powder X-ray diffraction measurements (Rigaku RINT2200) with CuKα radiation were also performed on shocked obsidian in the 2θ range of 5–50 ° with 0.01 °-step scan. These data were used to estimate the quantity of crystallites in obsidian.

Calculation of the radial distribution function (RDF)

The radial distribution function was calculated based on the procedure employed by Marumo and Okuno (1984). The measured X-ray scattering intensities were corrected for polarization, absorption factors, and Compton scattering factors (Levy et al. 1966). Compton scattering factors were calculated with the analytical formulas given by Hajdu (1971) and Pálinkás (1973). Normalization was carried out by Krogh–Moe's and Norman's method (Krogh–Moe 1956; Norman 1957). Atomic scattering factors were taken from the International Tables of X-ray Crystallography, vol. IV (1974). The composition of the obsidian used for the calculation was simplified to $Na_{0.332}K_{0.154}Ca_{0.060}Fe_{0.183}Al_{0.606}Si_{3.326}O_{8.000}$.

The X-ray interference function $S \cdot i(S)$ was calculated from the following expression,

$$S \cdot i(S) = S \cdot \left[I_{\mathrm{obs}}^{\mathrm{coh}}(S) - \sum_j f_j^2(S) \right] \Big/ \left\{ \sum_j f_j(S) \right\}^2 ,$$

where $f_j(S)$ is the atomic scattering factor of jth atom, and $I_{\mathrm{obs}}^{\mathrm{coh}}(S)$ is the total coherent intensity per electron unit.

The radial distribution function RDF(r) is given by the following formula,

$$\mathrm{RDF}(r) = 4\pi r^2 \rho_0 + \frac{2r}{\pi} \left(\sum_j \overline{K}_j \right)^2 \int_0^{S_{\max}} S \cdot i(S) \sin(Sr) dS ,$$

where ρ_0 is the number of formula unit per $Å^{-3}$ and $\overline{K}_j$ is the effective number of electrons for atom j.

Raman and infrared spectroscopy

Raman spectra were recorded by micro-Raman spectrometers, LabRamHR800 (Jobin Yvon) of HORIBA Jobin Yvon and

Ramanor T-64000 (Jobin Yvon) of Japan Advanced Institute of Science and Technology. The 514.5-nm line (green) of the Ar^+ laser was used to excite Raman scattering, and the Raman light was collected in the backscattering geometry. Spectra were accumulated in the range of 200–1400 cm^{-1} with a band pass of 0.5 cm^{-1}.

Observed Raman spectra were corrected for background, and the temperature and frequency dependence of the first-order (Stokes) Raman scattering (Long 1977; Piriou and Alain 1979; McMillan et al. 1994) from the expression:

$$I_{\mathrm{corr}} = I_{\mathrm{obs}}\omega(\omega_0 - \omega)^{-4}[1 - \exp(-h\omega/k_B T)] \ ,$$

where ω_0 is the wavenumber of the incident laser light (19435 cm^{-1} for the green Ar^+ laser line), h is the Plank's constant, ω is the Raman shift, k_B is Boltzmann's constant (1.36×10^{-23} JK^{-1}), and T is the absolute temperature (K).

The IR absorption measurements were performed by the KBr micropellet method using FT/IR-610V (JASCO) equipped with a KBr beam splitter and a TGS detector. Spectra were recorded from 400–5000 cm^{-1} with a band pass of 0.5 cm^{-1}.

Results

Density

The density variations of the obsidian and its fused glass with applied shock pressure are listed in Tables 2 and 3 and also plotted in Fig. 1. The densification of obsidian and its fused glass increased rapidly with shock pressures above ~15 GPa and reached a maximum (4.7% for obsidian; 3.6% for fused glass) at about 25 GPa. This is followed by a rapid reduction in density at higher shock pressures. At about 35 GPa, the density of fused glass dropped to almost the same density as the unshocked sample. The density of obsidian at 36.8 GPa is slightly lower than the unshocked obsidian, and similar to that of fused glass.

Table 2 Densities of shock-compressed obsidians

Shock pressure (GPa)	Density (g cm^{-3})	Densification (%)
Unshocked	2.409(3)	–
16.3	2.431(3)	0.91
21.7	2.503(4)	3.90
24.3	2.522(4)	4.69
31.0	2.436(10)	1.12
36.8	2.390(4)	−0.79

Table 3 Densities of shock-compressed fused glasses

Shock pressure (GPa)	Density (g cm^{-3})	Densification (%)
Unshocked	2.379(3)	–
15.2	2.392(6)	0.55
19.4	2.458(2)	3.32
25.9	2.465(3)	3.61
30.9	2.388(7)	0.38
35.1	2.377(3)	−0.10

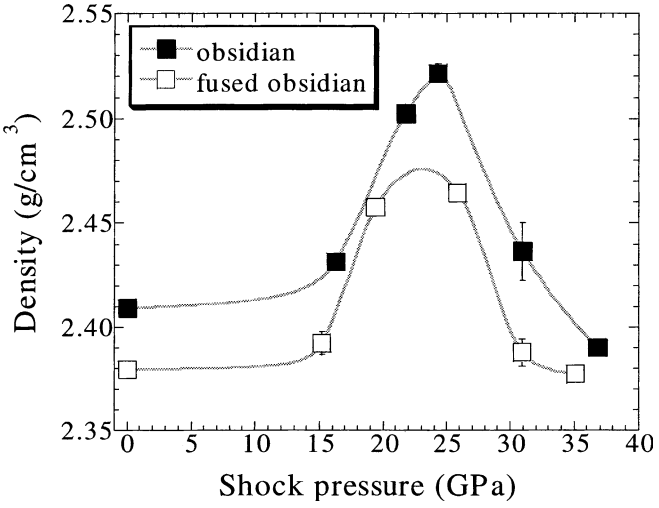

Fig. 1 Density variations of an obsidian and its fused glass by shock-wave compression. The gray lines are a guide for eyes

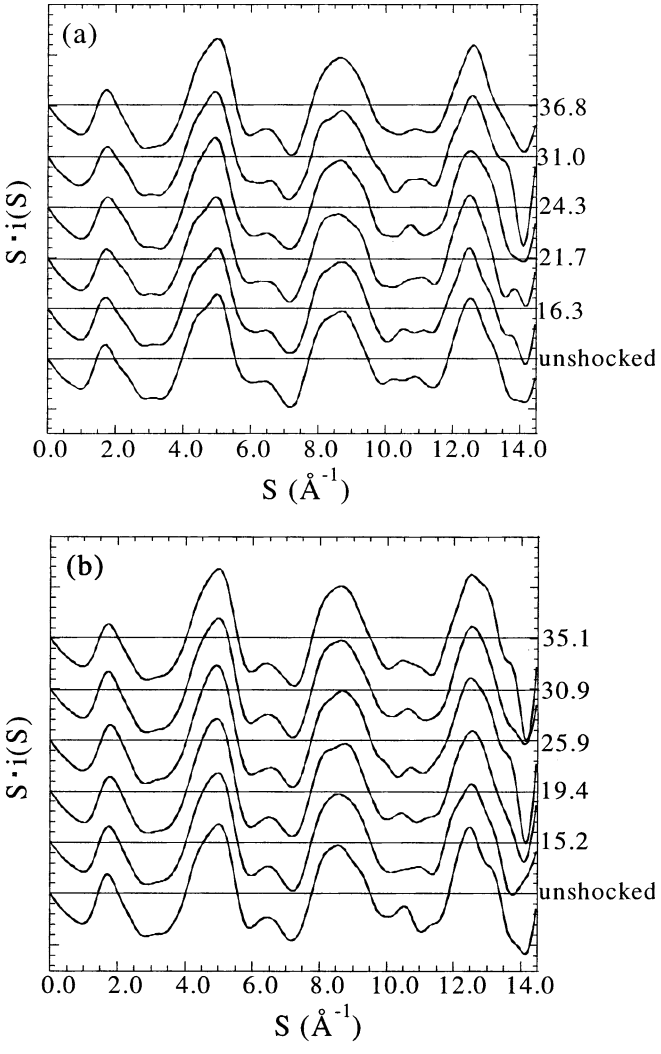

Fig. 2a–b $S \cdot i(S)$ curves for unshocked and shocked obsidian (**a**) and fused glass. (**b**) Numbers represent shock pressures in GPa

X-ray diffraction analysis

The interference functions $S \cdot i(S)$ is for obsidian and fused obsidian are shown in Fig. 2a and b, respectively. These curves are essentially similar in shape. Prominent peaks in their RDF(r) curves (Fig. 3a, b) can be seen at ~1.6 and 3.1 Å. These peaks are attributed to T–O1 distance (T = Si, Al) in a TO_4 tetrahedron and T–T1 distance between neighboring tetrahedra, respectively. The shoulder at around 2.6 Å is assigned to the O–O1 pair within a TO_4 tetrahedron, but can include small contributions from (Na, K, Ca)–O1 pairs. Broad peaks at 4.2 and 5.1 Å are attributed to T–O2 and T–T2 pair distance of the dominant six-membered ring, respectively (Hochella and Brown 1984; Zotov et al. 1989, 1992). The number of oxygen atoms around a T atom was calculated to be 4.0 ± 0.2 from the area under the first peak ($r = 1.63$ Å) in the RDF(r) curves. An average T–O–T angle of 147.0° ± 2.0° was obtained for all the samples. These suggest that the T atoms are tetrahedrally coordinated by oxygens in the structures of both normal and shock-densified obsidian and fused glass.

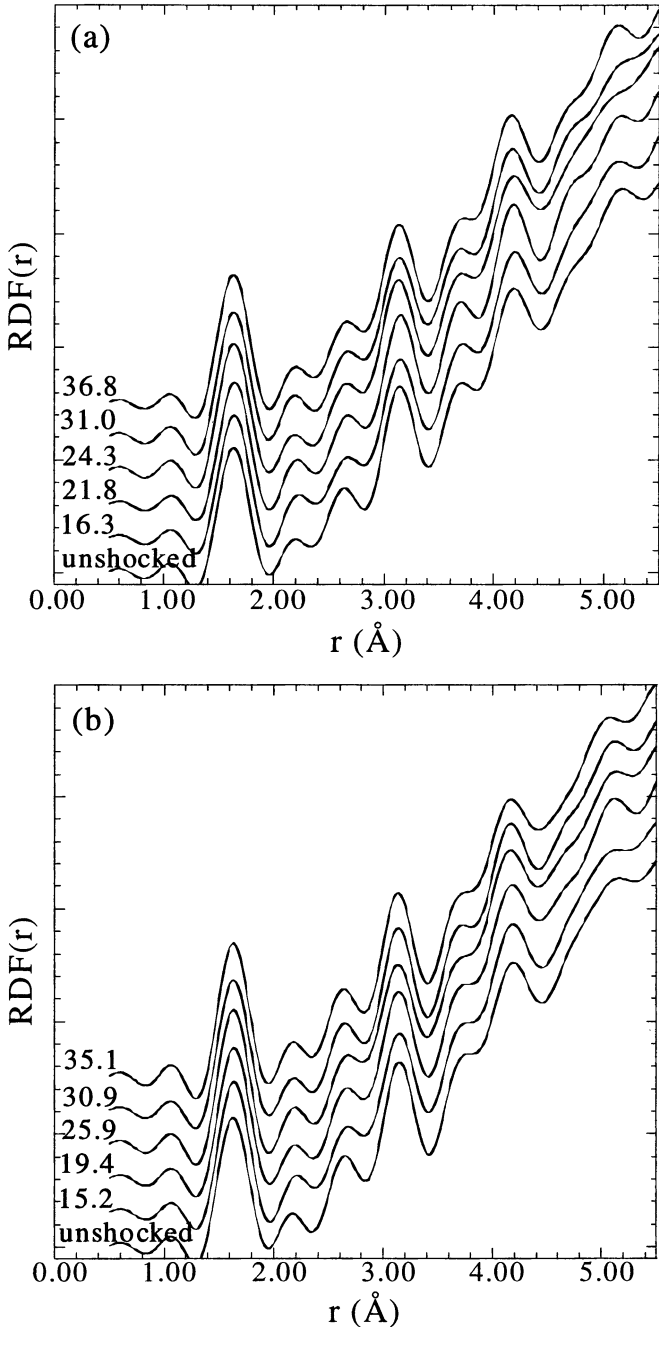

Fig. 3a,b Radial distribution functions for unshocked and shocked obsidian (**a**) and funsed glass. (**b**) Numbers represent shock pressures in GPa

Analysis of Raman spectra

The Raman spectra of shock-densified obsidian and fused glass are shown in Fig. 4a and b, respectively. Typical broad bands are observed at 300–600, 800, and 1000–1200 cm^{-1} for both specimens. An additional sharp band at around 670 cm^{-1} is observed only in obsidian specimens.

The band assignments of Raman spectra are explained based on the previous works on SiO_2-rich glasses (McMillan 1984; McMillan and Wolf 1995; Okuno et al. 1999; Reynard et al. 1999). The broad band centered at 490 cm^{-1} is attributed to the bending vibration of the T–O–T linkage in the tetrahedral framework. A small contribution from the oxygen-breathing mode of the four-membered ring of TO_4 tetrahedra is possible, which is generally located at 490 cm^{-1}. The shoulder at around 600 cm^{-1} in fused glasses is attributed to oxygen-breathing vibration of the three-membered ring of the TO_4 terahedra. A corresponding shoulder also appears in the lower frequency tail (550–600 cm^{-1}) of 670-cm^{-1} band of the obsidian. The band at 800 cm^{-1} is assigned to in-cage motion of silicon atoms in the highly polymerized network. Furthermore, the band at 1000–1200 cm^{-1} is attributed to antisymmetric T–O stretching vibration. The strong 670-cm^{-1} band for obsidian can be attributed to the crystalline parts (crystallites) of the obsidian, although it cannot be clearly determined (Okuno et al. 1998). It should also be noted that there is a slight difference in the 1000 cm^{-1} band between the obsidian and fused obsidian. The relatively sharp peak at 1000 cm^{-1} in obsidian samples can also be due to crystallites. The broad 490 cm^{-1} band in Fig. 4 shows a positive frequency shift while the intensity of the 600-cm^{-1} band varies with pressure above 25–30 GPa.

Analysis of IR spectra

The IR spectra of shock-densified obsidian and its fused glass are shown in Fig. 5a and b. Three major bands can be seen at 460, 780, and 1060 cm^{-1}. These bands are assigned to O–T–O bending vibration (460 cm^{-1}), symmetric T–O stretching (780 cm^{-1}), and antisymmetric

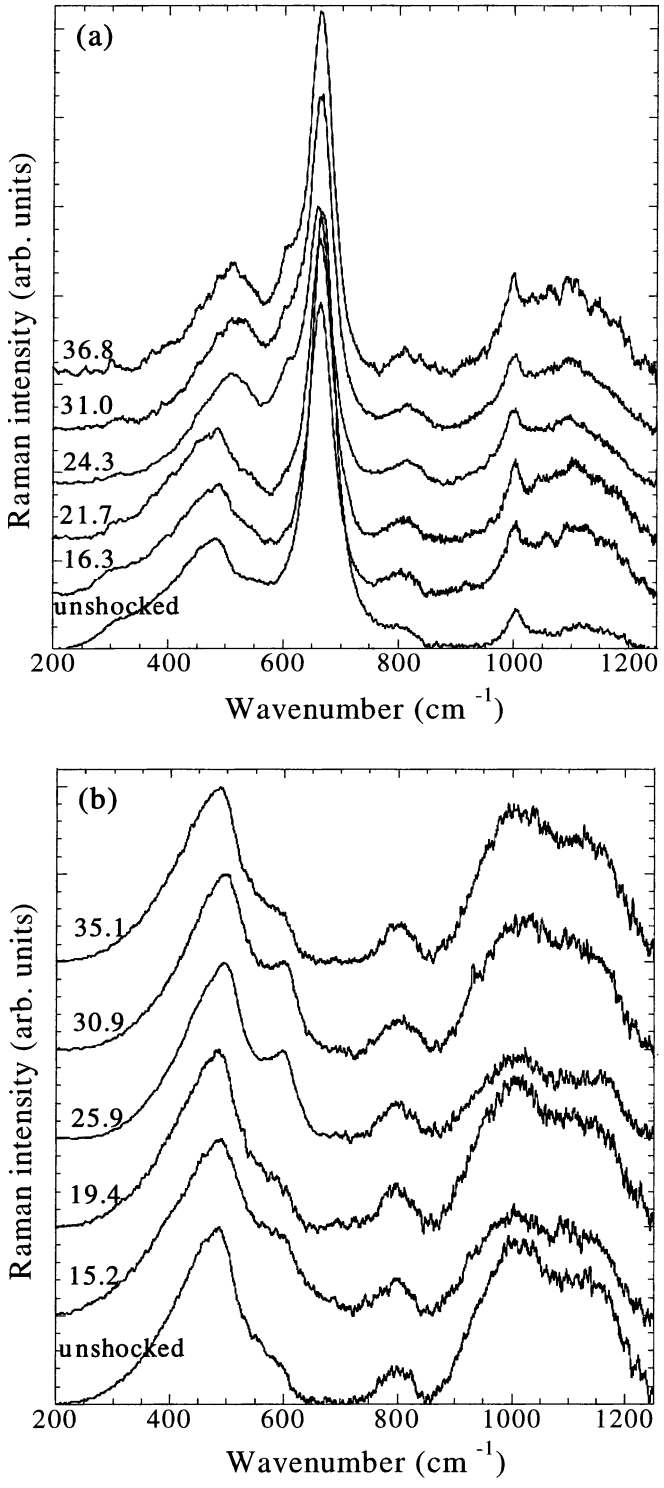

Fig. 4a,b Raman spectra for unshocked and shocked obsidian (**a**) and fused glass (**b**) Note that these spectra are representative ones among several data acquistitions. Numbers represent shock pressures in GPa

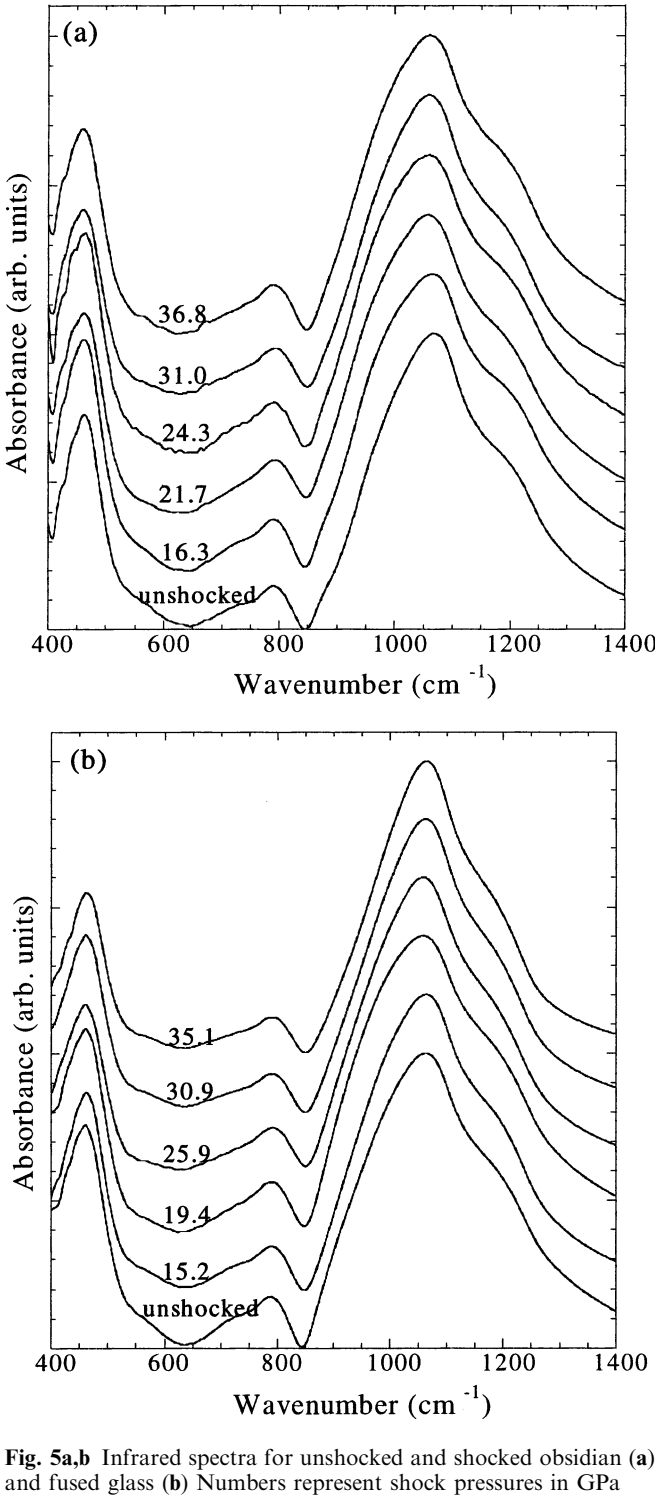

Fig. 5a,b Infrared spectra for unshocked and shocked obsidian (**a**) and fused glass (**b**) Numbers represent shock pressures in GPa

T–O stretching vibration (1060 cm^{-1}), according to Velde and Couty (1987). There are no significant differences in the spectra between obsidian and its fused glass, nor changes with shock pressure.

Discussion

Density variations with shock pressure

The density variations in obsidian and its fused glass with shock pressure are shown in Fig. 1. Both specimens show an increase in density and a subsequent reduction with

respect to shock pressure. A similar trend in density variation was observed in shock-compressed SiO_2 and feldspar glasses (Arndt et al. 1971; Okuno et al. 1999; Reynard et al. 1999; Takabatake 2000). The first regime in the density variation involves an increase in density with shock pressure up to 25 GPa, and is related to the densification of the structure. A second regime involves the relaxation of the densified structure at even higher shock pressure (>25 GPa) due to high residual temperature, which is observed as the subsequent decrease in density.

Gibbons and Ahrens (1971) have previously reported the variations in the refractive index of tektite glass effected by shock compression up to 13.3 GPa. Below 4 GPa, the refractive index of the tektite glass does not differ significantly with the unshocked glass. At 8 GPa, the refractive index grew and reached a maximum at 13.3 GPa. The refractive index increase, designated $(n_{13.3}\text{-}n_0)/n_0$, was found to be 2.38%. In this expression, $n_{13.3}$ and n_0 are the refractive indices for the 13.3-GPa-recovered and unshocked glass, respectively. Although the measurements made by Gibbons and Ahrens (1971) span only up to 13.3 GPa, their results are qualitatively consistent with the results in the present study.

The density variations in obsidian and its fused glass with shock pressure are similar to those of silica (Okuno et al. 1999), anorthite (Reynard et al. 1999), and albite (Takabatake 2000) glasses. Figure 6 shows density differences of shocked obsidian and its fused glass in comparison with those obtained in previous studies. The maximum densifications of shock-densified silica, anorthite, and albite glasses are 11.0, 2.2, and 4.2%, respectively at shock pressure of ~25 GPa. The differences in maximum densification could be due to the differences in the original glass structure (Reynard et al. 1999). The maximum densification values of shock-densified obisidian (4.7%) and fused obsidian (3.6%) suggest that the structural features of obsidian and its fused glass are similar to albite glass. This is consistent with the CIPW norm minerals calculated for this obsidian (i.e., albite + orthoclase = ~50 wt%). Taylor and Brown (1979) reported that alkali feldspar glasses had "stuffed-tridymite-like" structure, which consisted of six-membered rings of TO_4 tetrahedra and interstitial modifier cations (i.e., Na^+, K^+). These results further suggest that the obsidian and its fused glass also have "stuffed-tridymite-like" structure with dominant six-membered rings of TO_4 tetrahedra and interstitial modifier cations, which is similar to the suggestion of Hochella and Brown (1984). The interstitial cations can also hinder the puckering of the silicate framework and lead to the differences in the maximum densifications.

Okuno et al. (1998) investigated the structural evolution of an obsidian similar to the specimen used in the present study under hydrostatic compression of 4 GPa and 500°C. The reported permanent densification of about 9% (2.63 gcm^{-3}) is twice as great as the maximum densification determined in this study despite a lower pressure applied. The discrepancy in the densification from shock- and static-recover experiments could be due to the post-shock annealing and differences in the duration of compression applied. According to previous studies (Anderson et al. 1998; Okuno et al. 1999; Reynard et al. 1999; Takabatake 2000), the post-shock residual temperature of 900–1000°C can be estimated at

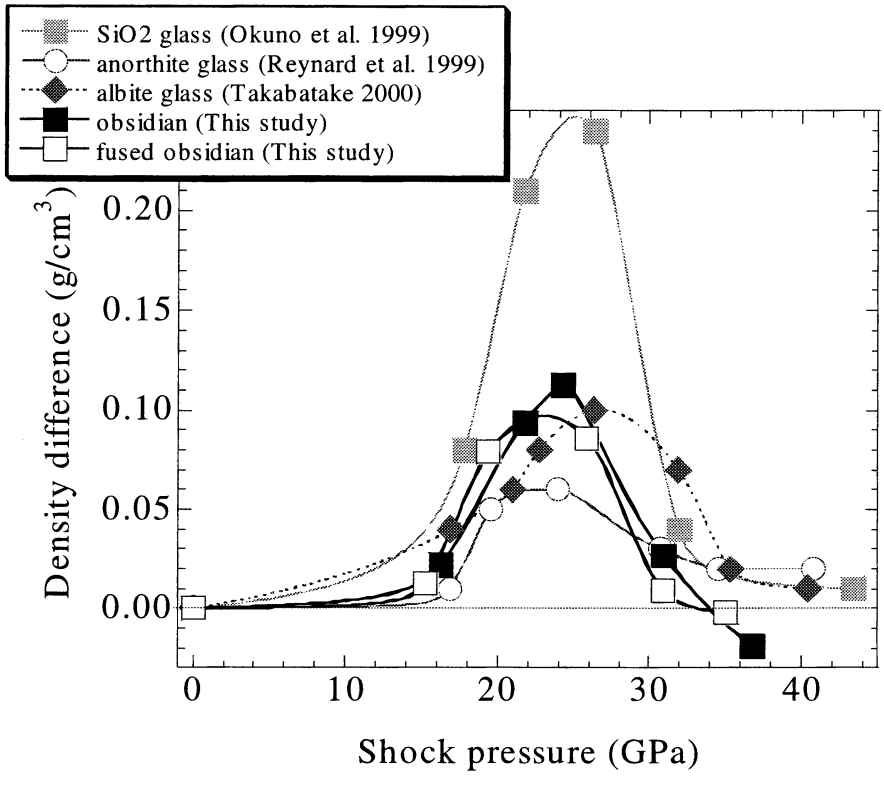

Fig. 6 Density differences between shocked and unshocked specimens of obsidian and fused glass as a function of shock pressure. The previous data for SiO_2, albite, anorthite glasses are also compiled for comparison. Solid squares obsidian; open squares fused glass; gray squares SiO_2 glass by Okuno et al. (1999); open circle anorthite glass by Reynard et al. (1999); dark gray diamond albite glass by Takabatake (2000). Lines are a guide for eyes

~35 GPa for obsidian, which is equivalent to the glass transition temperature of the obsidian.

Structural evolution in shock-densified obsidian and its fused glass

RDF(r) cures in Fig.3 have similar shapes and the T–O1 distances for all samples are about 1.63 Å. This is close to the average distance of the SiO_4 and AlO_4 tetrahedra (Si–O = 1.61 Å, Al–O = 1.74 Å; Whittaker and Muntus 1970), and to the estimated distance from an empirical equation by Zotov et al. (1989, 1992). The average T–O–T angle of 147° is consistent with the previous works for feldspar glasses (Taylor and Brown 1979a) and volcanic glass (Okuno et al. 1996; Zotov et al. 1992). In addition, the presence of peaks at about 4.2 and 5.1 Å indicates the predominance of a six-membered ring in the obsidian structure, which had been predicted by other authors (Hochella and Brown 1984; Okuno et al. 1996, 1998). Since no distinction can be made regarding pressure variations in the RDF(r) curves, structural changes of shock-densified obsidian and fused obsidian cannot be determined from the RDF(r) curves.

The T—O distances and coordination numbers did not change in the shock-densified obsidian and its fused glass, consistent with the previous studies on silica and feldspar glasses (Okuno et al. 1999; Reynard et al. 1999; Takabatake 2000; Shimada et al. 2002). This indicates that the TO_4 tetrahedra in the structures are retained after shock recovery and that the density variations of shock-densified obsidian and fused glass cannot result from the coordination change of the tetrahedral cations (Si, Al). However, Meade et al. (1992), using in situ diamond-anvil cell technique, found that the Si–O distance and the coordination number increased with pressure up to 42 GPa. Anderson et al. (1998) pointed out that a transition region mixed with low-pressure and high-pressure phases existed in the range of 9 to 34 GPa upon examination of the pressure–volume Hugoniot data obtained for rhyolite. It implies that highly coordinated T (T = Si, Al) species, formed under shock state, may revert to a four-coordinated configuration during decompression (Gibbons and Ahrens 1971). The reversion of the coordination state can occur due to post-shock annealing.

Recent studies have interpreted the structural evolution of densified silica glass in terms of the first sharp diffraction peak (FSDP) from X-ray structure factor curves (Susman et al. 1990; Tan and Arndt 1999; Shimada et al. 2002). Using the concept of quasi-lattice, FSDP position (S_1) can be associated to the averaged cell dimension, d_m ($d_m = 2\pi/S_1$), of medium-range structural units (e.g., ring structure of TO_4 tetrahedra). Figure 7 shows the variation of FSDP position for shock-densified obsidian and fused glass extracted by the polynomial fitting procedure. The FSDP moves to higher S values with shock pressure up to ~25 GPa and retraces to lower values with higher pressure. With

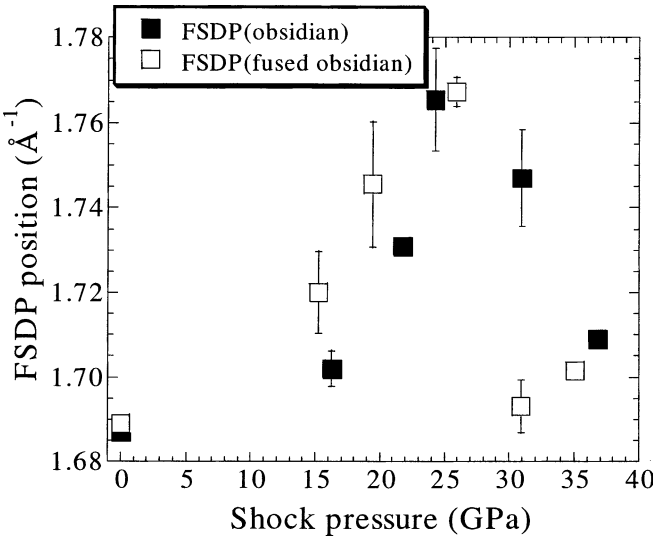

Fig. 7 The variations of FSDP position for obsidian and its fused glass as a function of pressure

respect to FSDP and the average ring distribution of TO_4 tetrahedra, Susman et al. (1990) and Shimada et al. (2002) insisted that the migration of FSDP position to higher S in the densified glass indicated an increase in the population of smaller rings (i.e.,three-, or four-membered rings). The population of small rings increased with applied shock pressure up to ~25 GPa but decreased at higher pressures because of the relaxation due to high post-shock temperature (Okuno et al. 1999).

Shimada et al. (2002) observed a pressure-induced maximum shift of 0.14Å^{-1} in the FSDP position for shocked silica glass. In the present study, the maximum FSDP shift is 0.08Å^{-1} for both shocked obsidian and fused glass. The FSDP positions for unshocked obsidian and fused glass ($S_1 = 1.69$Å^{-1} for both samples) were found higher than for unshocked silica glass[1.56 Å^{-1}, re-extracted from $i(S)$ of Shimada et al. 2002] and close to albite glass (1.66Å^{-1}). This suggests a larger amount of small rings in the obsidian or rhyolitic glass than in the structure of silica glass. It is also supported by the prediction that the AlO_4 tetrahedra energitic prefer to form small rings (Kubicki and Sykes 1993; Sykes and Kubicki 1996).

Raman spectra for shock-compressed obsidian and its fused glass also show clear pressure variations. For obsidian, the frequency of the broad band at 490 cm^{-1} shows a positive shift (22 cm^{-1}) from 484 to 506 cm^{-1} with increasing shock pressure up to 31.0 GPa, and a subsequent reduction to 493 cm^{-1} at 36.8 GPa (Fig.8). In the same manner, for fused obsidian a positive shift from 480 to 495 cm^{-1} with shock pressure up to 25.9 GPa and a subsequent reduction to 486 cm^{-1} at 35.1 GPa are observed, as shown in Fig.8. This band is assigned to the T–O–T-bending mode of the TO_4 network structure. Since this band is related to the average T–O–T angle, a positive frequency shift with shock pressure means a reduction of the average T–O–T angle

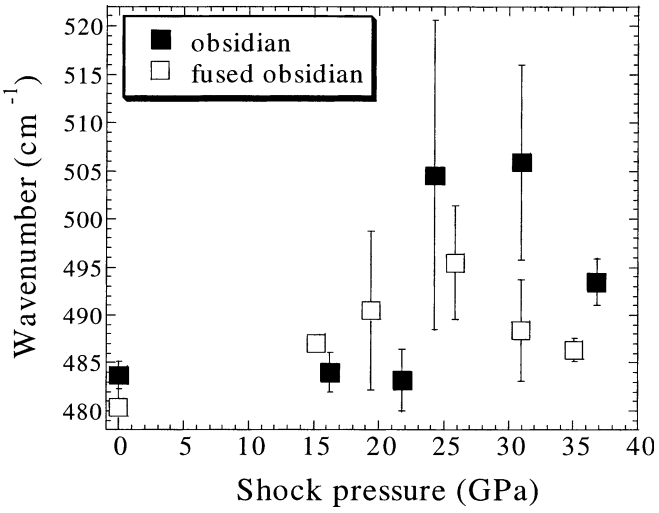

Fig. 8 Frequency variations of the broad 490 cm^{-1} band in Raman spectra as a function of shock pressure. Solid squares obsidian; open squares fused glass. A polynominal fitting was used for extracting band top positions. The fitting precision is within 2 cm^{-1}. The error bars mean the standard deviation from several spectra

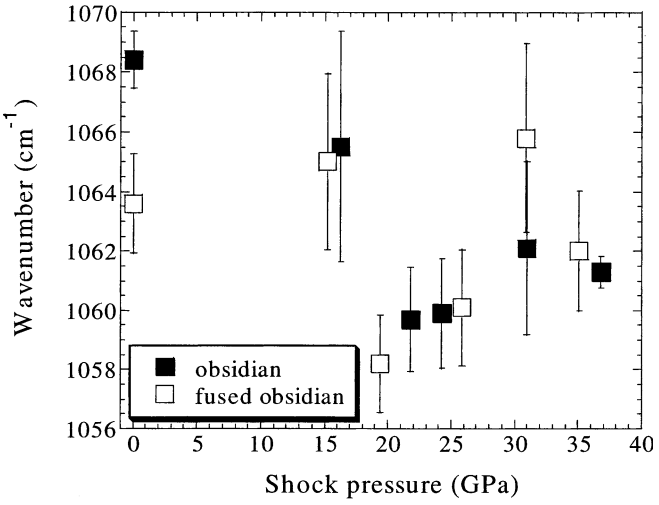

Fig. 9 Frequency variations of the T–O-stretching vibration centered at 1060 cm^{-1} in IR spectra. Solids squares obsidian; open squares fused glass. The data points were extracted simply from the band top positions. The error bars mean the standard deviation from several spectra

(McMillan et al. 1984; Wolf and McMillan 1995). Okuno et al. (1999) reported the corresponding band shift for shock-densified silica glass to be 48 cm^{-1} (from 457 to 505 cm^{-1}). The difference in frequency shift between shock-densified obsidian, fused glass, and silica glass is consistent with the difference in maximum densification (obsidian 4.7%, fused glass 3.6%, and silica glass 11.0%). Assuming that the frequency change associated with the Si–O–Si bond angle reduction was about 5.5 cm^{-1} per degree (Okuno et al. 1999), the positive shifts of 22 and 15 cm^{-1} for obsidian and fused glass correspond to the reduction in T–O–T angle by 4.0° and 2.7°, respectively. These values are reasonably small to be examined by RDF analysis. It should be noted that the frequency variations of this T–O–T-bending mode (maximum at 31.0 GPa) do not seem to be strictly correlated to density variations (maximum at 24.3 GPa) for shock-densified obsidian, although large standard deviations observed at 24.3 and 31.0 GPa (Fig. 8) make that unclear. For fused glass, the frequency variations of the T–O–T-bending mode follow the density variations. This difference in pressure response between obsidian and fused obsidian cannot be easily explained. However, it may be influenced by the overlap with the 670-cm^{-1} band in obsidian.

The IR band at 1060 cm^{-1} in both samples corresponding to T–O antisymmetric stretching shifts to lower frequency with increasing shock pressure to 20–25 GPa (Fig.9). This indicates a slight lengthening of the T–O bond distance and gives indirect evidence for the reduction of the mean T–O–T angle (Lasaga and Gibbs 1988; Murray and Ching 1989).

The pressure variation of the 600 cm^{-1} band intensity is observed in Raman spectra. This variation is quite unclear for obsidian due to the overlap with the 670-cm^{-1} band. On the contrary, the intensity increase of the 600-cm^{-1} band at 25–30 GPa and the decrease at 35.1 GPa are observed for fused glass. This indicates the increase of the three-membered ring during shock compression of 25–30 GPa and the subsequent reduction due to high post-shock temperature at higher pressure (Okuno et al. 1999).

Tektites are theorized to form by shock compression during a meteorite impact. Wright et al. (1984) reported that obsidian and tektite have similar structural features and differ slightly from silica glass with respect to medium-range ordering, based on the results by neutron diffraction analyses. White and Minser (1984) examined Raman spectra of obsidian and tektite, and showed their spectral similarity. These findings suggest that the structure of tektite is similar to that of volcanic glasses such as obsidian. Giuli et al. (2000) have recently shown that Al atoms in tektite are tetrahedrally coordinated based on the Al K-edge XANES spectra. Our results also suggest that Al atoms are oxygen-coordinated in a tetrahedral manner in all shock-recovered samples. Based on the findings in the present study, tektites possibly have experienced shock-melting under high residual temperatures resulting from shock compression above 35 GPa by meteorite impacts.

The structural evolutions of obsidian and its fused glass during shock compression are summarized from the above discussions as follows:

1. The density increase up to shock pressures of ~25 GPa results from the shrinkage of the TO_4 tetrahedral framework structure (the reduction of T–O–T bond angle), ~ and an increase in the small rings of TO_4 tetrahedra (i.e., three- and four-membered rings);
2. A high residual temperature promotes the relaxation of the compressed network above 25 GPa (i.e., increase in the average T–O–T bond angle and partial relaxation of small rings), which results in density reduction.

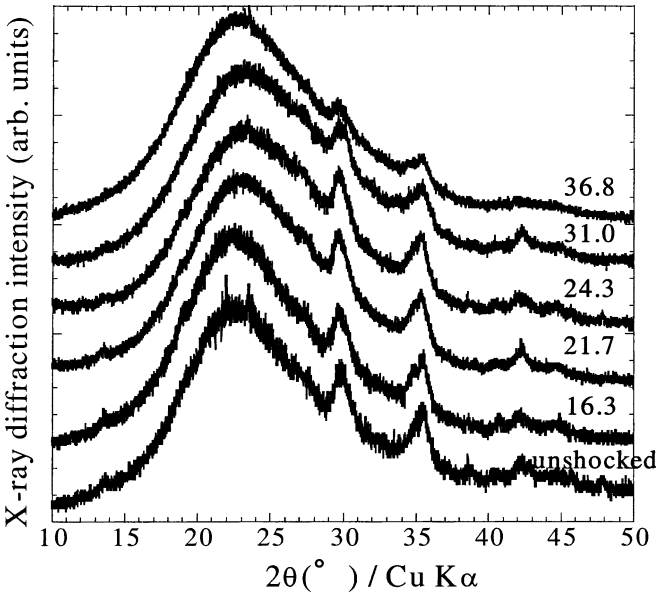

Fig. 10 X-ray diffraction patterns of shocked obsidian with Cukα radiation. Numbers represent shock pressures in GPa

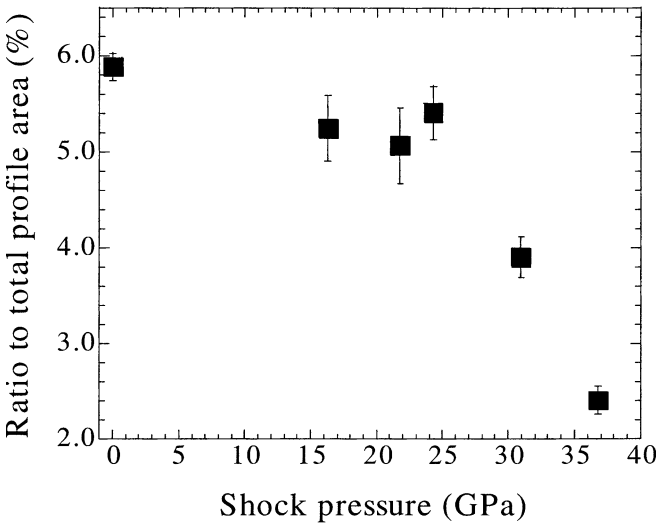

Fig. 11 Intensity variations of crystallite peaks as a function of shock pressure for obsidian. The vertical axis shows the percentage of the crystallite peak areas with respect to total profile areas in 2θ range of 10°–40°

Pressure variation of crystallites

The prominent 670 cm^{-1} band in the Raman spectra of natural obsidian (Fig. 4a) is not observed nor in that of fused glass (Fig.4b), nor in other silicate glasses studied by other authors (i.e., Okuno et al. 1999; Reynard et al. 1999; Takabatake 2000, etc.) Okuno et al. (1998) suggested that this band possibly corresponded to the presence of crystallites. It was also observed that the intensity of this band decreased variably with shock pressure above 25–30 GPa, which could be associated with crystallite orientation. Tattevin et al. (1990) reported that a distinct pressure response develops with different crystal orientation.

Pressure-induced changes in the quantity of the crystallites were investigated with powder X-ray diffractometer using a CuKα radiation source. Diffraction profiles obtained from CuKα radiation were more sensitive to crystallites than when using a MoKα radiation source. The X-ray diffraction patterns for shocked obsidian have a broad peak at around $2\theta = 23°$ associated with the glass matrix in the obsidian structure (Fig.10). There are two other prominent sharp peaks at $2\theta = 29.9°$ and 35.1°, which can be due to crystallites. These peaks were not observed in the diffraction patterns for fused glass. Figure 11 shows the sum of the intensity variations of these two peaks as a function of shock pressure These figures show a rapid reduction in intenstiy and line broadening of the two peaks above 25 GPa.

Lambert (1981) showed a rapid reduction in the refractive indices of several silicate crystals due to amorphization with shock pressure above 25 GPa. Since the refractive index is correlated with density (Okuno et al. 1999; Reynard et al. 1999), the density of the crystalline phase decreases rapidly by shock compression above 25 GPa and reaches the value of the amorphous phase. These facts suggest that crystallites in the obsidian begin amorphization by shock compression above 25 GPa. The observed lower density of shock-compressed obsidian at 36.8 GPa (2.39 gcm^{-3}) compared to the unshocked obsidian (2.41 gcm^{-3}) and close to fused obsidian (2.38 gcm^{-3}) can be explained by density reduction of crystallites due to shock-induced amorphization. Using the procedure of Zotov et al. (1989), the predicted quantity of crystallites in the unshocked obsidian (0.8 wt% with a precision of 0.1 wt%) was reduced after shock compression of 36.8 GPa (0.3 wt%). This prediction agrees qualitatively with a density gap between unshocked obsidian and fused glass (Δ = 1.3%), and between the 36.8-GPa shocked obsidian and the 35.1-GPa shocked fused glass (0.4%).

The present study has shown that obsidian and its fused glass have essentially the same structural features and undergo similar structural evolutions with applied shock compression. The presence of crystallites only contributes to the density of the obsidian.

Conclusions

The structural evolutions of obsidian and its fused glass by shock-wave compression can be summarized as follows:

The densities of obsidian and its fused glass increase with applied shock pressure up to about 25 GPa. The maximum densification determined for obsidian and its fused glass are 4.7 and 3.6%, respectively. These values are close to the shock-densified feldspar glasses (2–4%). This reflects their structural similarity. Modifier cations in interstitial sites can prevent the large densification as in silica glass.

The pressure variations observed in the Raman spectra of obsidian and its fused glass indicate that the densification for shock pressure up to 25 GPa is mainly due to the reduction of the average T–O–T angle with a small contribution from an increase in the population of small rings such as three-, four-membered rings.

Partial relaxation of the densified structure due to relatively high residual temperature after shock-wave compression above 25 GPa results in the decrease in the densities of the obsidian and its fused glass.

At higher shock pressures (> 25 GPa), crystallites in the obsidian samples amorphize, which contributes to the density decrease. The presence of crystallites can influence the density variations; however, the small amount present (about 0.8 wt% of unshocked obsidian) did not significantly affect the differences in the structural evolutions of obsidian and its fused glass.

Findings of previous studies (Okuno et al. 1999; Takabatake 2000) are also confirmed in this study. This fact implies that the highly polymerized glasses have essentially similar shock-densification mechanisms, which can be slightly influenced by the existence of interstitial cations and by the ring distribution in the original structure.

Finally, our results also suggest that tektites have experienced shock-induced melting and subsequent rapid cooling with shock pressures greater than 35 GPa. Further works may still be needed to establish the structural relation between tektite and shocked obsidian.

Acknowledgements The authors would like to acknowledge Dr. Bruno Reynard of ENS Lyon for providing obsidian blocks. They also wish to express their thanks to Mr. Shoichi Okamoto and Ms. Tomoko Numata of HORIBA jovin Yvon Co. Ltd. for carrying out Raman spectra measurements. A part of this work was carried out under the Visiting Researcher's Program of the IMR, Tohoku University, Japan. This work was partly supported by a Grant-in-Aid for International Scientific Research (no. 09044069) of the Ministry of Education, Science, Sports, and Culture of Japan, by a Grant-in-Aid for Scientific Research (nos. 10440153 and 15340185) of the Japnese Society for the Promotion of Science (JSPS) and by the Foundation for Promotion of Material Science Technology of Japan (MST Foundation). Finally, the authors are indebted to referees for constructive suggestions and comments.

References

Anderson WW, Yang W, Chen G, Ahrens TJ (1998) Shock-wave equation of state of rhyolite. Geophys J Int 132: 1–13

Arndt J, Hornemann H, Müller WF (1971) Shock-wave densification of silica glass. Phys Chem Glasses 12: 1–7

Gibbons RV, Ahrens TJ (1971) Shock metmorphism of silicate glasses. J Geophys Res 76: 5489–5498

Giuli G, Pratesi G, Corazza M, Cipriani C (2000) Aluminium coordination in tektites: a XANES study. Am Mineral 85:1172–1174

Goto T, Syono Y (1984) Technical aspect of shock compression experiments using the gun method. In: Sunagawa I (ed) Material sciences of the earth's interior. Terra Scientific Publ Co, Tokyo, pp 65–619

Hadju F (1971) Analytic approximation for incoherent scattered X-ray intensities. Acta Crystallogr (A) 27: 73–74

Heide K, Heide G, Kloess G (2001) Glass chemistry of tektites. Planet Space Sci 49: 839–844

International tables for X-ray crystallography, vol. IV. (1974) kynoch press, Birmingham

Hochella MF, Brown GE Jr. (1984) Structure and viscosity of rhyolitic composition melts. Geochim Cosmochim Acta 48: 2631–2640

Krogh-Moe J (1956) A method for converting experimental X-ray intensities to an absolute scale. Acta Crystallogr 9: 951–953

Kubicki JD, Sykes D (1993) Molecular orbital calculations of vibrations in three-membered aluminosilicate rings. Phys Chem Miner 19: 381–391

Lambert P (1981) Reflectivity applied to peak pressure estimates in silicates of shocked rocks. J Geophys Res 86: 6187–6204

Lasaga AC, Gibbs GV (1988) Quantum mechanical potential surfaces and calculations on minerals and molecular clusters I. STO-3G and 6-31G* results. Phys Chem Miner 16: 29–41

Levy HA, Danford MD, Narten AH (1966) Data collection and evaluation with an X-ray diffractometer designed for the study of liquid structure. Oak Ridge National Laboratory Report 3960

Long DA (1977) Raman spectroscopy. McGraw Hill, London

Marumo F, Okuno M (1984) X-ray structural studies of molten silicates: anorthite and albite melts. In: Sunagawa I (ed), Material sciences of the Earth's interior. Terra Scientific, Tokyo, pp 25–38

McMillan P (1984) Structural studies of silicate glasses and melts: Applications and limitation of Raman spectroscopy. Am Mineral 69: 622–644

McMillan PF, Wolf GH (1995) Vibrational spectroscopy of silicate liquids. In: Stebbins JF, McMillan PF, Dingwell DB (eds), Structure, dynamics and properties of silicate melts. Reviews in Mineralogy, vol. 32, Mineralogical society of America Washington DC, pp 247–315

McMillan P, Piriou B, Couty R (1984) A Raman study of pressure-densified vitreous silica. J Chem Phys 81: 4234–4236

McMillan PF, Poe BT, Gillet PH, Reynard B (1994) A study of SiO_2 glass and supercooled liquid to 1950 k via high-temperature Raman spectroscopy. Geochim Cosmochim Acta 58: 3653–3664

Meade C, Hemley RJ, Mao HK (1992) High pressure X-ray diffraction of SiO_2 glass. Phys Rev Lett 69: 1387–1390

Murray RA, Ching WY (1989) Electronic- and vibrationl-structure calculation in models of the compressed SiO_2 glass systems. Phys Rev (B) 39: 1320–1331

Mysen BO, Virgo D, Seifert A (1982) The structure of silicate melts: implications for chemical and physical poperties of natural magma. Rev Geophys Space Phys 20: 353–383

Nakazawa S, Watanabe S, Kato M, Iijima Y, Kobayashi K, sekine T (1997) Hugoniot equation of state of basalt. Planet Space Sci 45: 1489–1492

Norman N (1957) A Fourier transformation method for normalizing intensities. Acta Crystallogr 12: 370–374

Okuno M, Iwatsuki H, Matsumoto T (1996) Structural analysis of an obsidian by X-ray diffraction method. Eur J Mineral 8: 1257–1264

Okuno M, Nakagami S, Shimada Y, Kusaba K, Syono Y, Ishizawa N, Yusa H (1998) Structural changes of a volcanic glass (obsidian) under high pressure. Rev High Pressure Sci Technol 7: 128–130

Okuno M, Reynard b, Shimada Y, Syono Y, Willaime C (1999) A Raman spectroscopic study of shock-wave densification of vitreous silica. Phys Chem Miner 26: 304–311

Pálinkás G (1973) Analytic approximation for the incoherenct X-ray intensities of atoms Ca to Am. Acta Crystallogr (A) 29: 10–12

Piriou B, Alain D (1979) Density states and structural form related structural properties of amorphous solids. High Temp High Press Res 11: 407–414

Reynard B, Okuno M, Shimada Y, Syono Y, Willaime C (1999) A Raman spectroscopic study of shock-wave densification of anorthite ($CaAl_2Si_2O_8$) glass. Phys Chem Miner 26: 432–436

Shimada Y, Okuno M, Syono Y, Kikuchi M, Fukuoka K, Ishizawa N (2002) An X-ray diffraction study of shock-wave-densified SiO_2 glasses. Phys Chem Miner 29: 233–239

Susman S, Volin KJ, Liebermann RC, Gwanmesia GD, Wang Y (1990) Structural changes in irreversibly densified fused glass: Implications for the chemical resistance of high-level nuclear waste glasses. Phys Chem Glass 31: 144–150

Sykes D, Kubicki JD (1996) Four-membered rings in silica and aluminosilicate glasses. Am Mineral 81: 265–272

Takabatake K (2000) Vitrification of albite crystal and structue change of albite glass by shock-wave compression. Master Thesis, Kanazawa University

Tan CZ, Arndt J (1999) X-ray diffraction of densified silica glass. J Non-Cryst Solids 249: 47–50

Tattevin H, Syono Y, Kikuchi M, Kusaba K, Velde B (1990) Shock deformation of alpha quartz: laboratory experiments and TEM investigation. Eur J Mineral 2: 227–234

Taylor M, Brown GE Jr. (1979) Structure of mineral glasses – I. The feldspar glasses $NaAlSi_3O_8$, $KAlSi_3O_8$, $CaAl_2Si_2O_8$. Geochim Cosmochim Acta 43: 61–75

Velde B, Couty R (1987) High pressure infrared spectra of some silicate glasses. Chem Geol 62: 35–41

White WB, Minser DG (1984) Raman spectra and structure of natural glasses. J Non-Cryst Solids 67: 45–59

Whittaker EJW, Muntus R (1970) Ionic radii for use in geochemistry. Geochim Cosmochim Acta 34: 945–956

Wright AC, Desa JAE, Weeks RA, Sinclair RN, Bailey DK (1984) Neutron diffraction studies of natural glasses. J Non-Cryst Solids 67: 35–44

Wolf GH, McMillan PF (1995) Pressure effects on silicate melt: Structure and properties. In: Stebbins JF, McMillan PF, Dingwell DB (eds), Structure, dynamics and properties of silicate melts. Reviews in Mineralogy 32 Mineralogical Society of America, Washington DC, pp 505–561

Zotov N, Dimitoriv V, Yanev Y (1989) X-ray radial distribution function analysis of acid volcanic glasses from the Eastern Rhodopes, Bulgaria. Phys Chem Miner 16: 774–782

Zotov N, Yanev Y, Epelbaum M, Konstantinov L (1992) Effect of water on the structure of rhyolite glasses — X-ray diffraction and Raman spectroscopy studies. J Non-Cryst Solids 142, 234–246